Fermi National Accelerator Laboratory

FERMILAB-Conf-96/183-E
D0

Direct Photon Measurements by the D0 Experiment

S. Abachi et al.
The D0 Collaboration

Fermi National Accelerator Laboratory
P.O. Box 500, Batavia, Illinois 60510

July 1996

Submitted at the *28th International Conference on High Energy Physics (ICHEP96)*,
Warsaw, Poland, July 25-31, 1996

Operated by Universities Research Association Inc. under Contract No. DE-AC02-76CHO3000 with the United States Department of Energy

Disclaimer

Direct Photon Measurements by the DØ Experiment

The DØ Collaboration[1]

(July 1996)

We report a measurement of the cross section for production of isolated photons with transverse energy $E_T > 12\ GeV$ in the central $|\eta| < 0.9$) and forward ($1.6 < |\eta| < 2.5$) rapididy regions for $\bar{p}p$ collisions at center of mass energy $\sqrt{s} = 1.8\ TeV$, using an integrated luminosity of 13 pb^{-1}. The cross section is compared with a next-to-leading order (NLO) QCD calculation. We also present preliminary measurements of the center of mass scattering angle distribution and of the correlations between the rapidity of the photon and that of the leading jet in the event.

S. Abachi,[14] B. Abbott,[28] M. Abolins,[25] B.S. Acharya,[43] I. Adam,[12] D.L. Adams,[37] M. Adams,[17] S. Ahn,[14] H. Aihara,[22] J. Alitti,[40] G. Álvarez,[18] G.A. Alves,[10] E. Amidi,[29] N. Amos,[24] E.W. Anderson,[19] S.H. Aronson,[4] R. Astur,[42] R.E. Avery,[31] M.M. Baarmand,[42] A. Baden,[23] V. Balamurali,[32] J. Balderston,[16] B. Baldin,[14] S. Banerjee,[43] J. Bantly,[5] J.F. Bartlett,[14] K. Bazizi,[39] J. Bendich,[22] S.B. Beri,[34] I. Bertram,[37] V.A. Bezzubov,[35] P.C. Bhat,[14] V. Bhatnagar,[34] M. Bhattacharjee,[13] A. Bischoff,[9] N. Biswas,[32] G. Blazey,[14] S. Blessing,[15] P. Bloom,[7] A. Boehnlein,[14] N.I. Bojko,[35] F. Borcherding,[14] J. Borders,[39] C. Boswell,[9] A. Brandt,[14] R. Brock,[25] A. Bross,[14] D. Buchholz,[31] V.S. Burtovoi,[35] J.M. Butler,[3] W. Carvalho,[10] D. Casey,[39] H. Castilla-Valdez,[11] D. Chakraborty,[42] S.-M. Chang,[29] S.V. Chekulaev,[35] L.-P. Chen,[22] W. Chen,[42] S. Choi,[41] S. Chopra,[24] B.C. Choudhary,[9] J.H. Christenson,[14] M. Chung,[17] D. Claes,[42] A.R. Clark,[22] W.G. Cobau,[23] J. Cochran,[9] W.E. Cooper,[14] C. Cretsinger,[39] D. Cullen-Vidal,[5] M.A.C. Cummings,[16] D. Cutts,[5] O.I. Dahl,[22] K. De,[44] M. Demarteau,[14] N. Denisenko,[14] D. Denisov,[14] S.P. Denisov,[35] H.T. Diehl,[14] M. Diesburg,[14] G. Di Loreto,[25] R. Dixon,[14] P. Draper,[44] J. Drinkard,[8] Y. Ducros,[40] S.R. Dugad,[43] D. Edmunds,[25] J. Ellison,[9] V.D. Elvira,[42] R. Engelmann,[42] S. Eno,[23] G. Eppley,[37] P. Ermolov,[26] O.V. Eroshin,[35] V.N. Evdokimov,[35] S. Fahey,[25] T. Fahland,[5] M. Fatyga,[4] M.K. Fatyga,[39] J. Featherly,[4] S. Feher,[14] D. Fein,[2] T. Ferbel,[39] G. Finocchiaro,[42] H.E. Fisk,[14] Y. Fisyak,[7] E. Flattum,[25] G.E. Forden,[2] M. Fortner,[30] K.C. Frame,[25] P. Franzini,[12] S. Fuess,[14] E. Gallas,[44] A.N. Galyaev,[35] T.L. Geld,[25] R.J. Genik II,[25] K. Genser,[14] C.E. Gerber,[14] B. Gibbard,[4] V. Glebov,[39] S. Glenn,[7] J.F. Glicenstein,[40] B. Gobbi,[31] M. Goforth,[15] A. Goldschmidt,[22] B. Gómez,[1] G. Gomez,[23] P.I. Goncharov,[35] J.L. González Solís,[11] H. Gordon,[4] L.T. Goss,[45] N. Graf,[4] P.D. Grannis,[42] D.R. Green,[14] J. Green,[30] H. Greenlee,[14] G. Griffin,[8] N. Grossman,[14] P. Grudberg,[22] S. Grünendahl,[39] W.X. Gu,[14,*] G. Guglielmo,[33] J.A. Guida,[2] J.M. Guida,[5] W. Guryn,[4] S.N. Gurzhiev,[35] P. Gutierrez,[33] Y.E. Gutnikov,[35] N.J. Hadley,[23] H. Haggerty,[14] S. Hagopian,[15] V. Hagopian,[15] K.S. Hahn,[39] R.E. Hall,[8] S. Hansen,[14] R. Hatcher,[25] J.M. Hauptman,[19] D. Hedin,[30] A.P. Heinson,[9] U. Heintz,[14] R. Hernández-Montoya,[11] T. Heuring,[15] R. Hirosky,[15] J.D. Hobbs,[14] B. Hoeneisen,[1,†] J.S. Hoftun,[5] F. Hsieh,[24] Tao Hu,[14,*] Ting Hu,[42] Tong Hu,[18] T. Huehn,[9] S. Igarashi,[14] A.S. Ito,[14] E. James,[2] J. Jaques,[32] S.A. Jerger,[25] J.Z.-Y. Jiang,[42] T. Joffe-Minor,[31] H. Johari,[29] K. Johns,[2] M. Johnson,[14] H. Johnstad,[29] A. Jonckheere,[14] M. Jones,[16] H. Jöstlein,[14] S.Y. Jun,[31]

[1]Submitted to the 28th International Conference on High Energy Physics, Warsaw, Poland, 25-31 July 1996.

C.K. Jung,[42] S. Kahn,[4] G. Kalbfleisch,[33] J.S. Kang,[20] R. Kehoe,[32] M.L. Kelly,[32] L. Kerth,[22] C.L. Kim,[20] S.K. Kim,[41] A. Klatchko,[15] B. Klima,[14] B.I. Klochkov,[35] C. Klopfenstein,[7] V.I. Klyukhin,[35] V.I. Kochetkov,[35] J.M. Kohli,[34] D. Koltick,[36] A.V. Kostritskiy,[35] J. Kotcher,[4] J. Kourlas,[28] A.V. Kozelov,[35] E.A. Kozlovski,[35] M.R. Krishnaswamy,[43] S. Krzywdzinski,[14] S. Kunori,[23] S. Lami,[42] G. Landsberg,[14] J-F. Lebrat,[40] A. Leflat,[26] H. Li,[42] J. Li,[44] Y.K. Li,[31] Q.Z. Li-Demarteau,[14] J.G.R. Lima,[38] D. Lincoln,[24] S.L. Linn,[15] J. Linnemann,[25] R. Lipton,[14] Y.C. Liu,[31] F. Lobkowicz,[39] S.C. Loken,[22] S. Lökös,[42] L. Lueking,[14] A.L. Lyon,[23] A.K.A. Maciel,[10] R.J. Madaras,[22] R. Madden,[15] L. Magaña-Mendoza,[11] S. Mani,[7] H.S. Mao,[14,*] R. Markeloff,[30] L. Markosky,[2] T. Marshall,[18] M.I. Martin,[14] B. May,[31] A.A. Mayorov,[35] R. McCarthy,[42] T. McKibben,[17] J. McKinley,[25] T. McMahon,[33] H.L. Melanson,[14] J.R.T. de Mello Neto,[38] K.W. Merritt,[14] H. Miettinen,[37] A. Mincer,[28] J.M. de Miranda,[10] C.S. Mishra,[14] N. Mokhov,[14] N.K. Mondal,[43] H.E. Montgomery,[14] P. Mooney,[1] H. da Motta,[10] M. Mudan,[28] C. Murphy,[17] F. Nang,[5] M. Narain,[14] V.S. Narasimham,[43] A. Narayanan,[2] H.A. Neal,[24] J.P. Negret,[1] E. Neis,[24] P. Nemethy,[28] D. Nešić,[5] M. Nicola,[10] D. Norman,[45] L. Oesch,[24] V. Oguri,[38] E. Oltman,[22] N. Oshima,[14] D. Owen,[25] P. Padley,[37] M. Pang,[19] A. Para,[14] C.H. Park,[14] Y.M. Park,[21] R. Partridge,[5] N. Parua,[43] M. Paterno,[39] J. Perkins,[44] A. Peryshkin,[14] M. Peters,[16] H. Piekarz,[15] Y. Pischalnikov,[36] V.M. Podstavkov,[35] B.G. Pope,[25] H.B. Prosper,[15] S. Protopopescu,[4] D. Pušeljić,[22] J. Qian,[24] P.Z. Quintas,[14] R. Raja,[14] S. Rajagopalan,[42] O. Ramirez,[17] M.V.S. Rao,[43] P.A. Rapidis,[14] L. Rasmussen,[42] S. Reucroft,[29] M. Rijssenbeek,[42] T. Rockwell,[25] N.A. Roe,[22] P. Rubinov,[31] R. Ruchti,[32] J. Rutherfoord,[2] A. Sánchez-Hernández,[11] A. Santoro,[10] L. Sawyer,[44] R.D. Schamberger,[42] H. Schellman,[31] J. Sculli,[28] E. Shabalina,[26] C. Shaffer,[15] H.C. Shankar,[43] R.K. Shivpuri,[13] M. Shupe,[2] J.B. Singh,[34] V. Sirotenko,[30] W. Smart,[14] A. Smith,[2] R.P. Smith,[14] R. Snihur,[31] G.R. Snow,[27] J. Snow,[33] S. Snyder,[4] J. Solomon,[17] P.M. Sood,[34] M. Sosebee,[44] M. Souza,[10] A.L. Spadafora,[22] R.W. Stephens,[44] M.L. Stevenson,[22] D. Stewart,[24] D.A. Stoianova,[35] D. Stoker,[8] K. Streets,[28] M. Strovink,[22] A. Sznajder,[10] P. Tamburello,[23] J. Tarazi,[8] M. Tartaglia,[14] T.L. Taylor,[31] J. Thompson,[23] T.G. Trippe,[22] P.M. Tuts,[12] N. Varelas,[25] E.W. Varnes,[22] P.R.G. Virador,[22] D. Vititoe,[2] A.A. Volkov,[35] A.P. Vorobiev,[35] H.D. Wahl,[15] G. Wang,[15] J. Warchol,[32] G. Watts,[5] M. Wayne,[32] H. Weerts,[25] A. White,[44] J.T. White,[45] J.A. Wightman,[19] J. Wilcox,[29] S. Willis,[30] S.J. Wimpenny,[9] J.V.D. Wirjawan,[45] J. Womersley,[14] E. Won,[39] D.R. Wood,[29] H. Xu,[5] R. Yamada,[14] P. Yamin,[4] C. Yanagisawa,[42] J. Yang,[28] T. Yasuda,[29] P. Yepes,[37] C. Yoshikawa,[16] S. Youssef,[15] J. Yu,[14] Y. Yu,[41] Q. Zhu,[28] Z.H. Zhu,[39] D. Zieminska,[18] A. Zieminski,[18] E.G. Zverev,[26] and A. Zylberstejn[40]

[1] Universidad de los Andes, Bogotá, Colombia
[2] University of Arizona, Tucson, Arizona 85721
[3] Boston University, Boston, Massachusetts 02215
[4] Brookhaven National Laboratory, Upton, New York 11973
[5] Brown University, Providence, Rhode Island 02912
[6] Universidad de Buenos Aires, Buenos Aires, Argentina
[7] University of California, Davis, California 95616
[8] University of California, Irvine, California 92717
[9] University of California, Riverside, California 92521
[10] LAFEX, Centro Brasileiro de Pesquisas Físicas, Rio de Janeiro, Brazil
[11] CINVESTAV, Mexico City, Mexico
[12] Columbia University, New York, New York 10027
[13] Delhi University, Delhi, India 110007
[14] Fermi National Accelerator Laboratory, Batavia, Illinois 60510
[15] Florida State University, Tallahassee, Florida 32306
[16] University of Hawaii, Honolulu, Hawaii 96822
[17] University of Illinois at Chicago, Chicago, Illinois 60607

[18]Indiana University, Bloomington, Indiana 47405
[19]Iowa State University, Ames, Iowa 50011
[20]Korea University, Seoul, Korea
[21]Kyungsung University, Pusan, Korea
[22]Lawrence Berkeley National Laboratory and University of California, Berkeley, California 94720
[23]University of Maryland, College Park, Maryland 20742
[24]University of Michigan, Ann Arbor, Michigan 48109
[25]Michigan State University, East Lansing, Michigan 48824
[26]Moscow State University, Moscow, Russia
[27]University of Nebraska, Lincoln, Nebraska 68588
[28]New York University, New York, New York 10003
[29]Northeastern University, Boston, Massachusetts 02115
[30]Northern Illinois University, DeKalb, Illinois 60115
[31]Northwestern University, Evanston, Illinois 60208
[32]University of Notre Dame, Notre Dame, Indiana 46556
[33]University of Oklahoma, Norman, Oklahoma 73019
[34]University of Panjab, Chandigarh 16-00-14, India
[35]Institute for High Energy Physics, 142-284 Protvino, Russia
[36]Purdue University, West Lafayette, Indiana 47907
[37]Rice University, Houston, Texas 77251
[38]Universidade Estadual do Rio de Janeiro, Brazil
[39]University of Rochester, Rochester, New York 14627
[40]CEA, DAPNIA/Service de Physique des Particules, CE-SACLAY, France
[41]Seoul National University, Seoul, Korea
[42]State University of New York, Stony Brook, New York 11794
[43]Tata Institute of Fundamental Research, Colaba, Bombay 400005, India
[44]University of Texas, Arlington, Texas 76019
[45]Texas A&M University, College Station, Texas 77843

I. INTRODUCTION

Direct photons permit clean tests of the predictions of QCD. At leading order, photon production directly probes the partonic interaction, without the ambiguities associated with jet identification, fragmentation and jet energy measurement. The dominant modes of production are from gluon-quark and quark-quark scattering. The former process makes the outgoing photon a useful probe of the incoming gluon.

II. DETECTOR AND EVENT SELECTION

Photons are identified in the DØ detector (1) using a uranium/liquid argon sampling calorimeter. The electromagnetic section covers the region of pseudorapidity $|\eta| < 3$ (where $\eta = -\ln\tan\frac{\theta}{2}$) with energy resolution $\sigma_E/E = 15\%/\sqrt{E(\mathrm{GeV})} \oplus 0.3\%$, and position resolution ~ 2 mm. The calorimeter is divided into four longitudinal layers (EM1–EM4) of 2, 2, 7 and 10 radiation lengths respectively; the transverse segmentation in pseudorapidity and azimuthal angle is into towers of $\Delta\eta \times \Delta\phi = 0.1 \times 0.1$ (0.05×0.05 in EM3). Drift chambers before the calorimeter allow photons to be distinguished from electrons and photon conversions by dE/dx measurement.

Data are recorded using a three-level triggering system. At the first level, signals are required in a scintillator counter near the beam pipe, which detects an inelastic $p\bar{p}$ interaction. The next level is a fast hardware trigger which sums the electromagnetic energy in

calorimeter towers of size $\Delta\eta \times \Delta\phi = 0.2 \times 0.2$. The data used in this analysis correspond to 13 pb^{-1} of integrated luminosity recorded during the 1992–93 collider run. They were taken with transverse energy thresholds of 2.5, 7, and 10 GeV. The third level is a software trigger in which clusters of calorimeter cells are formed and loose cuts made on shower shape. The thresholds used at this level were 6, 14, and 30 GeV.

Additional cuts are applied to the photon candidates off-line. Candidates and their associated isolation cone ($R = \sqrt{\Delta\eta^2 + \Delta\phi^2} = 0.4$) were restricted to fully instrumented regions of the calorimeter. The electromagnetic energy fraction of the calorimeter shower was required to be greater than 96% and the shower shape was required to be consistent with the shape of test beam electrons. The photons were required to be isolated by a cut on the transverse energy in a region between $R = 0.2$ and $R = 0.4$ around the photon: $E_T^{R=0.4} - E_T^{R=0.2} < 2\ GeV$. Finally, the missing transverse energy $E_T^{\rm miss}$ of the event is required to be less than 20 GeV to reject electrons from $W \to e\nu$ decays and events with large amounts of calorimeter noise.

III. BACKGROUND ESTIMATION

The primary experimental challenge in the measurement of the direct photon cross section is the extraction of the prompt photon signal from the copious backgrounds due to π^0 and η mesons produced in jets and subsequently decaying to photons. The bulk of this jet background is rejected by the selection criteria listed above, especially by the requirement that the photon candidates be isolated; but substantial contamination remains from fluctuations in the jet fragmentation, which lead to a meson carrying most of the jet's energy. In the E_T range covered by this experiment, the two photons from meson decay coalesce (most of the time) and mimic a single photon shower in the calorimeter. Fluctuations in the shower development make background subtraction on an event-by-event basis impossible. We have therefore subtracted the remaining background on a statistical basis.

The fraction of candidates fulfilling the selection criteria which are genuine direct photons (the purity $\mathcal{P}$) was determined using the energy E_1 deposited in the first layer (EM1) of the calorimeter. Neutral meson decays produce two photons, and so the probability that at least one of them undergoes a conversion to an e^+e^- pair in the calorimeter cryostat and first absorber plate is roughly twice that for a single photon. Meson showers therefore start earlier than photon showers, leading to larger E_1. As a discriminant, we use the variable $\log(E_1/E_{\rm total})$ as shown in Fig. 1. The distribution is fit as the sum of Monte Carlo generated photon signal plus π^0 and η meson backgrounds. Fitting was done separately for the central and forward samples for each E_T^γ bin, using χ^2 minimization, and constraining the fractions of signal and background to lie in the range $[0, 1]$. The results presented use a production ratio of $\eta/\pi^0 = 1.0\ (4)$, but all values between 0.50 and 1.25 give essentially indistinguishable results for $\mathcal{P}$, since the distributions of $\log(E_1/E_{\rm total})$ for π^0 and η mesons are similar after cuts. The Monte Carlo calculation combines a detailed simulation of the calorimeter with overlaid minimum bias events from data to model noise, pileup and the underlying event. Its ability to correctly model the $E_1/E_{\rm total}$ distribution has been verified using samples of electrons from $W \to e\nu$ events taken with the same trigger requirements.

The combined statistical and systematic error on the purity $\mathcal{P}$, at each E_T^γ point was estimated by inflating the fitting error by $\sqrt{\chi^2/DoF}$ for that E_T. The multiplicative factor accounts for systematic differences between the Monte Carlo distributions and the data. It was typically 1.3 in the central region and 1.6 in the forward region. The central and forward photon purities were then corrected by the E_T-dependent efficiencies and fit to the form: $\mathcal{P} = 1 - e^{-(a+bE_T^\gamma)}$. The data points, fits, and fit errors for $\mathcal{P}$ are shown in Fig.1.

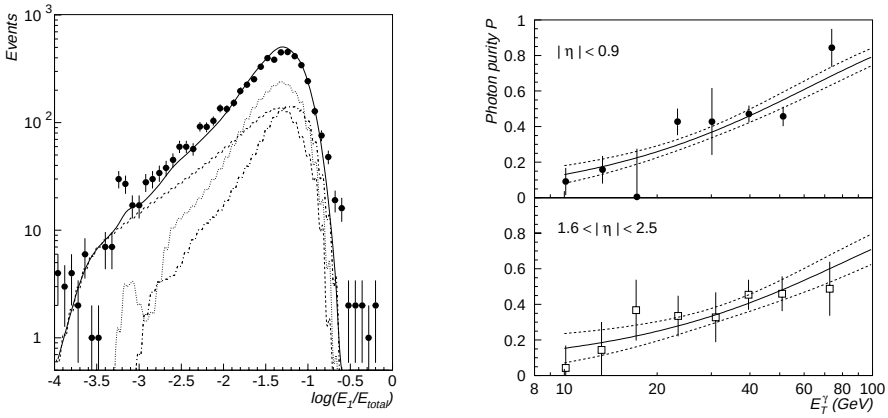

FIG. 1. (left) Histogram of the discriminant variable $log(E_1/E_{\rm total})$, solid line is the result of the fit to and admixture of γ(dot-dot), π^0(dash-dash), and η(dot-dash) components. (right) The photon Purity/efficiency vs. Transverse Energy. The errors shown are combined statistical and systematic; the lines indicate the fit and its variation.

A second method of background subtraction was used to check the results from the calorimeter energy deposition method. It also takes advantage of the difference in conversion probability between single photons and background. In this case, the material between the interaction point and the drift chamber causes conversions which are measured with twice minimum ionizing energy using the drift chambers. The results from the two methods were found to be consistent in the central region. The conversion method has larger statistical errors (only 10% of photons convert) and therefore is not used in the fit.

IV. INCLUSIVE CROSS SECTION

Figure 2 (left) shows a plot of $(\sigma_e - \sigma_t)/\sigma_t$ where σ_e and σ_t are the experimental and theoretical cross sections respectively. The error bars on the data points reflect the statistical uncertainty only. The shaded band in Fig. 2 (left) shows the total correlated systematic uncertainly from all sources including $\pm 5\%$ normalization uncertainty from the luminosity. The theoretical cross section is the next-to-leading order QCD calculation of Baer *et al.* (2) using CTEQ2M parton distributions (3) with a renormalization scale $\mu = E_T$. The theoretical calculation has been smeared with the experimental electromagnetic energy resolution, and includes an isolation requirement to match that used in the experimental analysis.

Because of our unique measurement of the cross section in the forward rapidity region, it is possible to plot the ratio of forward to central cross sections which allows for cancellation of the luminosity uncertainty. This is shown in Fig. 2 (right) along with the NLO prediction, as a function of scaled transverse energy $x_T = 2E_T^\gamma/\sqrt{s}$.

V. ANGULAR DISTRIBUTION

The inclusive cross section is a convolution of matrix elements and parton distributions. Information about the matrix elements alone can be obtained by measuring the angular distribution in the CM frame. In order to be able to reconstruct the kinematics of the event in the CM frame, it is also necessary to know the direction of the recoiling jets.

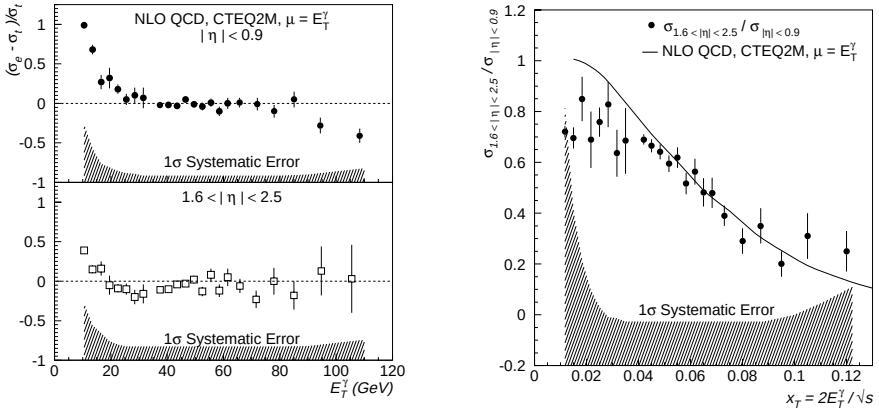

FIG. 2. (left) Comparison between data and NLO QCD theory, using CTEQ2M parton distributions; (right) The ratio of forward to central cross sections vs. scaled transverse energy x_T.

Therefore we require at least one jet which passes standard cuts (which remove isolated noisy calorimeter cells and main ring losses) be found in the event, and that the total missing-$E_T < 0.3E_T^\gamma$. To retain the simplicity of the $2 \rightarrow 2$ process, all jets in the opposite hemicylinder from the photon, are combined to form the photon recoil object. The quantities measured are the photon transverse energy and rapidity and the rapidity obtained from the vector sum of all jets opposite the photon. The CM quantities are then given by: $\eta^* = \frac{\eta_\gamma - \eta_{jet}}{2}$, $\eta_{boost} = \frac{\eta_\gamma + \eta_{jet}}{2}$, $E^* = E_T^\gamma cosh\eta^*$, and $cos\theta^* = tanh\eta^*$.

This analysis requires $E_T^\gamma > 30\ GeV$ and $|\eta_\gamma| < 0.9$, and $|\eta_{jet}| < 3.0$. To avoid acceptance corrections, only events in the three regions shown in Fig. 3 (left) are used in the analysis. These regions each cover a range of 0.8 in η^* and η_{boost}. Furthermore, the photon CM energy is required to be above the trigger threshold: $E^* > E_T^\gamma cosh\eta^*_{max}$. The raw distribution is formed by adding events from the three regions, with the constraint that regions higher in η_{jet} be normalized in the overlap region. The result is a distribution that has the shape of the signal and background. Rather than compute an angle dependent photon purity, the shape of the background is obtained from a pure sample of jets with $E_T > 30\ GeV$. Photons were required to pass the same set of selection cuts as the inclusive sample, so the purity ($\mathcal{P}$) $\sim$ 50%. The background was then subtracted using the purity as the relative normalization. The preliminary results are shown in Fig 3 (right) along with the results from a previous measurement (5) and the NLO prediction. Both results show good agreement with the theory.

VI. PHOTON-JET RAPIDITY CORRELATIONS

Since the dominant direct photon production process at the Tevatron is gluon Compton scattering, an analysis of the rapidity correlation between the photon and the leading jet can provide information about the gluon distributions of the colliding hadrons. Specifically, when one fixes the angle of the photon, one can probe a range of parton momenta by looking at the angular distribution of the leading associated jet. In the following preliminary analysis the η^{jet} distributions are determined for several ranges of photon rapidity η^γ.

A sample of photon candidates was selected from data taken during the 1994–95 run with an integrated luminosity of 35 pb^{-1}. Standard photon identification cuts were applied.

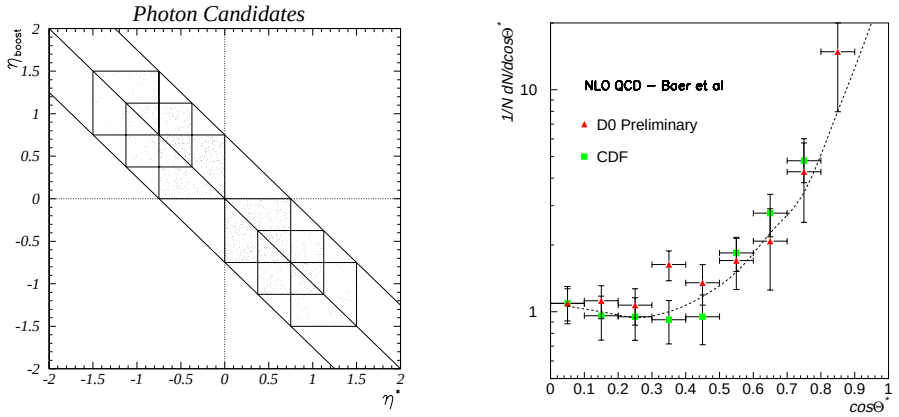

FIG. 3. (left)Distribution of candidates in η_{boost} and η^* for the regions used. (right) Plot of the normalized $cos\theta^*$ cross section for both DØ and CDF compared to the normalized NLO prediction. Only statistical errors are shown for both experiments.

Photons were allowed in both central ($|\eta_\gamma| < 0.9$) and forward ($1.5 \leq |\eta_\gamma| < 2.5$) regions of the detector. The transverse energy of the photon was required to be greater than 45 GeV. Lastly, the ratio of energy in the first electromagnetic layer to the total shower energy was required to be less than 1%. This cut was applied in order to increase the photon purity in the sample: about 75% of the resulting events are expected to be genuine isolated photons.

In this analysis, events were binned in five ranges of absolute photon rapidity $|\eta^\gamma|$. The "signed" pseudorapidity of the leading jet, η^{jet} (positive if in the same rapidity direction as the photon and negative if opposite) was then plotted. These distributions are shown in Fig. 4. The data show a tendency for the leading jet to follow the photon candidate forward, though not fully. The average pseudorapidity of the leading jet is indicated in the figure for each of the $|\eta^\gamma|$ regions.

As an estimate of the behavior of the background, a sample was created which was expected to discriminate *against* photons. Both the isolation and the longitudinal energy deposition cuts were reversed (isolation $> 2\,\mathrm{GeV}$, $E_1/E_{total} > 1\,\%$) and one or more of other cuts expected to enhance the jet background were also required (two or more tracks in front of the EM cluster, increased hadronic energy, non-photon-like shower shape). This background sample is expected to be dominated by jets with a large electromagnetic component. The correlation of the pseudorapidity of the leading jet with the rapidity of this fake photon sample is also shown in Fig. 4. There is a much less pronounced tendency for the leading jet to follow the EM jet (background) forward. To cross check the behavior of the background sample, events in this sample were compared with a sample of dijet events. The two samples gave consistent results.

Figure 5 summarizes the different behavior of the sample enriched with photon-jet events and that dominated by jet-jet background. The prediction of NLO QCD (2) for photon-jet events is also shown in Fig. 5 and is in good qualitative agreement with the data (though it does not include any admixture of jet-jet background).

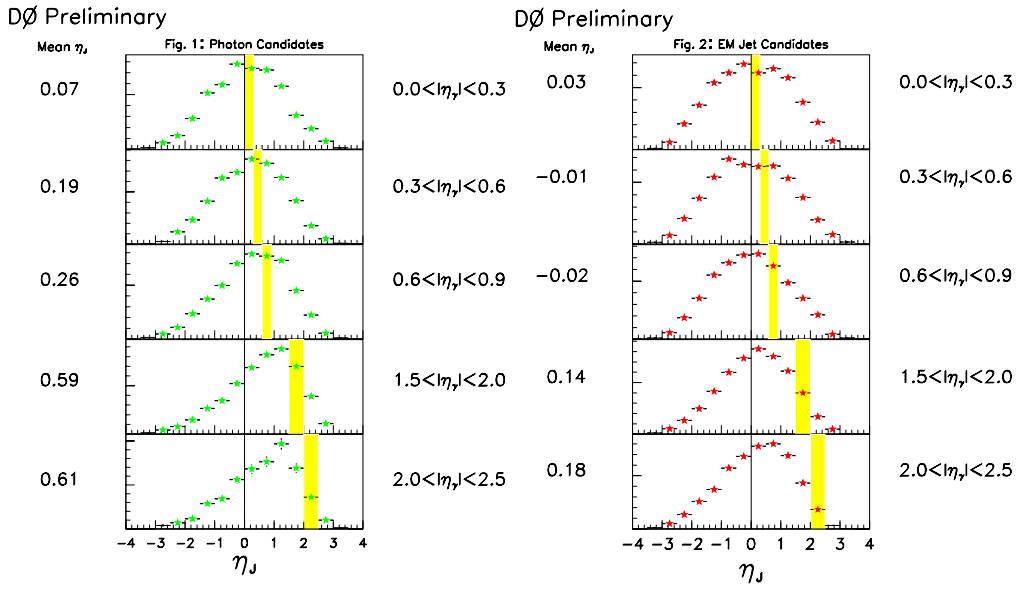

FIG. 4. Distributions of η^{jet} for five different regions of $|\eta^\gamma|$: (left) photon candidates, (right) jet-jet dominated sample. The shaded band shows the region of $|\eta^\gamma|$.

VII. CONCLUSIONS

We have measured the cross section of single isolated photons produced in $p\bar{p}$ collisions at $\sqrt{s} = 1.8TeV$. It is found to be in good agreement with the predictions of next-to-leading-order QCD for $E_T^\gamma > 30\,\mathrm{GeV}$ in both the forward and central rapidity regions. Below this value of E_T^γ the cross sections show large deviations from the QCD prediction; however, large systematic errors arising from split neutral meson clusters prohibit any conclusive statement at this time. It should be noted that similar effects have been observed by other experiments (4,6) in the low-E_T^γ range, and an ad-hoc theoretical explanation has been proposed which requires NLO QCD and additional initial state parton showers (7). The center of mass scattering angle distributions have also been measured and are consistent with NLO QCD. The correlation between leading jet rapidity and photon rapidity has been studied and is found to be in qualitative agreement with the NLO QCD prediction, while a jet-jet sample exhibits distinctly different behavior.

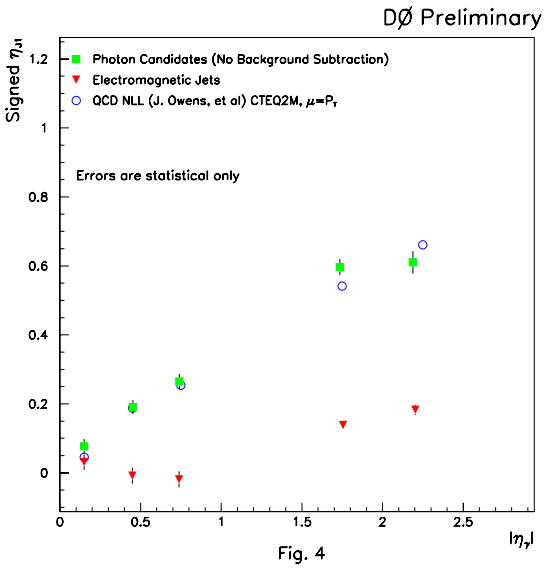

Fig. 4

FIG. 5. The mean of the η^{jet} distribution as a function of $|\eta^{\gamma}|$ for photon candidates, for the jet-jet dominated sample, and the NLO QCD prediction for photon events.

ACKNOWLEDGMENTS

We thank the staffs at Fermilab and the collaborating institutions for their contributions to the success of this work, and acknowledge support from the Department of Energy and National Science Foundation (U.S.A.), Commissariat à L'Energie Atomique (France), Ministries for Atomic Energy and Science and Technology Policy (Russia), CNPq (Brazil), Departments of Atomic Energy and Science and Education (India), Colciencias (Colombia), CONACyT (Mexico), Ministry of Education and KOSEF (Korea), CONICET and UBACyT (Argentina), and the A.P. Sloan Foundation.

REFERENCES

* Visitor from IHEP, Beijing, China.
† Visitor from Univ. San Francisco de Quito, Ecuador.

1. S. Abachi *et al.*, *Nucl. Instr. and Meth.* **A338** (1994) 185.
2. H. Baer, J. Ohnemus, J.F. Owens, *Phys. Rev.* **D42** (1990) 61.
3. J. Botts *et al.*, *Phys. Lett.* **B304** (1993) 159.
4. F. Abe *et al.*, *Phys. Rev. Lett.* **71** (1993) 679.
5. F. Abe *et al.*, *Phys. Rev. Lett.* **71** (1993) 680.
6. J. Alitti *et al.*, *Phys. Lett.* **B236** (1991) 544.
7. H. Baer and M.H. Reno, *hep-ph/9603209*, 1 March 1996.